Heliyon 10 (2024) e39291

Contents lists available at ScienceDirect

Heliyon

journal homepage: www.cell.com/heliyon

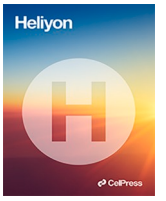

Research article

Zuogui Jiangtang Jieyu prescription improves diabetes-related depression by modulation of gut microbiota and neuroinflammation in hippocampus

Li Wei, Yang Hui, Wang Jinxi, Lei Shihui, Long Hongping, Liu Jian, Liu Lin *

Medical Innovation Experimental center, The First Hospital of Hunan University of Chinese Medicine, Changsha, Hunan, China

ARTICLE INFO

Keywords:
Zuogui Jiangtang Jieyu prescription
Gut microbiota
16S rRNA
Inflammation
TLR4/MyD88

ABSTRACT

Context: There is a significant challenge associated with the co-morbidity of mental and physical illnesses throughout the world. A classic example of mental/physical co-morbidity is diabetes-related depression (DD).
Objective: DD is treated with Zuogui Jiangtang Jieyu prescription (ZJJ). Diabetes and psychiatric disorders are associated with dysbiosis of the gut microbiota. In this study, the aim is to examine the effects of ZJJ on gut microbiota and neuroinflammation in DD.
Methods: A model of DD was established and treated with medium and high doses of ZJJ as well as Metformin & Fluoxetine. A detection of depressive-like behavior was then conducted on the rats. Proinflammatory cytokines were measured in cerebrospinal fluid, and HPA axis-related proteins, glucose metabolism, and lipopolysaccharide (LPS) were measured in serum. Fecal samples from each group were collected and analyzed by 16S rRNA sequencing; TLR4 and MyD88 levels were detected by Western blot and immunohistochemistry (IHC) in the hippocampus.
Results: High doses of ZJJ (ZJJ-H) were found to alleviate HPA axis hyperactivity and improve gut microbiota in rats with DD. Additionally, ZJJ treatment attenuated the inflammatory response in cerebrospinal fluid, e.g. a significant reduction in proinflammatory factors, a decrease in serum LPS levels, and an inhibition of TLR4/MyD88-related pathways in the hippocampus.
Discussion and conclusion: ZJJ improved DD glucose metabolism and alleviated depression-like behaviors by improving gut microbiota and inhibiting hippocampal TLR4/Myd88 signaling pathways.

1. Introduction

It is estimated that 643 million people worldwide will live with diabetes in 2030, according to the International Diabetes Federation. Depression is two to three times more likely to affect diabetics than healthy people, and depression can further exacerbate type 2 diabetes (T2DM) [1] and result in diabetes-related depression (DD). This disease will result in more serious complications as a result of its unstable blood sugar, serious effect on quality of life, increased mental burden, and other factors, resulting in a threefold increase in mortality [2]. It is therefore of great importance to study the pathogenesis of DD in order to prevent and treat it accordingly.

Diabetes-related depression (DD) has recently been linked to gut microbiota disorders [3,4]. Previous studies have demonstrated

* Corresponding author.
E-mail address: 286410883@qq.com (L. Lin).

https://doi.org/10.1016/j.heliyon.2024.e39291
Received 19 April 2024; Received in revised form 9 October 2024; Accepted 10 October 2024
Available online 15 October 2024

the influence of gut microbes on glucose metabolism [5]. The gut microbiota has also been demonstrated to play a role in the function of the central nervous system (CNS) [6], which has been linked to the development of depression [7]. Researchers have shown that gut mocriobiota can influence neuroimmune and neuroendocrine mechanisms through several microbial metabolites (such as short chian fat acids, secondary bile acids, and tryptophan metabolites, etc.), and subsequently control the central nervous system [8]. The activation of hippocampus microglia (MG) in DD can result in neuroinflammation [9]. TLR4/MyD88 signaling pathway has also been shown to be a classic inflammatory signaling pathway that is closely related to changes in gut microbiota in other studies [10]. It is unclear whether alterations in the gut microbiota affect neuroinflammation through regulation of the TLR4/MyD88 signaling pathway.

In the treatment and prevention of DD, hypoglycaemic drugs are typically combined with antidepressants, resulting in a number of side effects, frequent relapses, and poor patient compliance [11]. Traditional Chinese medicine (TCM) uses multiple approaches to regulate the whole body, including multiple links and multiple targets. There is an advantage to this medication in that it has a long-lasting effect and a low level of toxic side effects. Diabetes-related depressive symptoms have been successfully treated with the Zuigui Jiangtang Jieyu prescription (ZJJ). ZJJ was developed based on Zhang Jingyue's Zuo Gui drink and Zuo Gui pills. According to traditional Chinese medicine, ZJJ contains the following ingredients:Curcuma (Chinese name Jianghuang), Salvia miltiorrhiza (Chinese name Danshen), Achyranthes (Chinese name Niuxi), Lycium (Chinese name Gouqi), Astragalus mongholicus (Chinese name Huangqi), Paeonia × suffruticosa Andrews (Chinese name Mudanpi), Fructus corni (Chinese name Shanzhuyu), Eucommia ulmoidesc (Chinese name Duzhong), Cuscuta chinensis Lam (Chinese name Tusizi), Rehmannia glutinosa DC (Chinese name Shudihuang), Hypericum perforatum L (Chinese name Guanyelianqiao). The names of the plants have been verified through the website http://www.worldfloraonline.org/. A national patent has been granted for ZJJ (Patent No. CN101816766A). This formula contains Rehmannia glutinosa DC as a Jun to nourish kidney Yin. The Jun ministers, Fructus corni and Lycium, strengthen kidney Yin, while Cuscuta chinensis Lam, Achyranthes, and Eucommia ulmoides strengthen liver and kidney, Astragalus mongholicus enlivens spleen and benefits Qi, and Salvia miltiorrhiza and Paeonia × suffruticosa Andrews enhance blood flow. Moreover, Curcuma and Hypericum perforatum L were added in order to remove blood stasis and Qi, soothe the liver, and alleviate depression. Previous studies have demonstrated that it can reduce depression as well as increase blood sugar, blood lipids, and insulin levels in individuals with developmental disabilities [12]. Previous studies of our research group have confirmed that ZJJ can play a neuroprotective role by inhibiting the activation of hippocampal microglia (MG), improving neuroinflammation, and thereby increasing the expression of synapse-related proteins PSD95, SYN1 and BDNF in the hippocampus [9].

The purpose of this study was to examine the relationship between gut microbiota and DD, with or without treatment, using 16S rRNA sequences of fecal sample. In order to examine the advantages of ZJJ's multiple links and multiple targets, we examined whether ZJJ affects DD occurrence through the TLR4/MyD88 pathway, a classical inflammatory signaling pathway closely linked to gut microbiota changes. Providing new ideas for ZJJ treatment of DD by providing new targets.

2. Methods and materials

2.1. Animals

The rats used in this study were Sprague-Dawley rats (starting weight 200–220g) purchased from Hunan Slac Jingda Laboratory Animal Co., Ltd. (licence number SCXK 2009-0004). All rats were fed in a specific pathogen-free (SPF) laboratory at the First Hospital of Hunan University of Chinese Medicine. Animals were kept in a 12 h light/dark cycle (lights were turned on at 8:00 a.m.), at 22 °C with low humidity, and with access to food and water. Experiments involving animals were conducted in accordance with guidelines established by the National Institutes of Health (NIH publication 8023, revised 1996) and with the approval of the local Animal Use Committee (Approval No. ZYFY20211021-07).

2.2. Preparation of ZJJ and conditions of chromatographic and mass spectrometry

ZJJ was concentrated to 32.82 g kg^{-1} using a rotary evaporation apparatus for chromato-mass spectrometric analysis, preparation of drug-containing sera and in vitro intragastric administration.

Preparation of drug-containing serums: The dosage was 32.82 g kg^{-1} twice a day for five days. A serum sample was collected for analysis 1.5 h after the last dose.

Chromatography was performed using an Agilent ZORBAX Eclipse Plus C18 column (3.0 × 100 mm, 1.8 mm). The mobile phase was composed of organic acetonitrile (A) and aqueous phase (B), containing 1 % ammonium formate (mass spectrometry grade), and gradient elidation (0–5 min, 5%–15 % A; 5–10 min, 15%–35 % A; 10–20 min, 35%–65 % A); The flow rate was 0.4 mL per minute and the sample size was 2 L.

Mass spectrum conditions: positive and negative ion analysis were employed. The method of ionization is electrospray ionization (ESI). Agilent's standard tuning solution (G1969-85000) was used to obtain accurate mass number correction before injection analysis. The primary scanning detection range for mass spectrometry is $m.z^{-1}$ 100 1700; nitrogen is used to remove solvents during the drying process; the temperature of the system is 325 °C. Flow rate was 6.8 L min^{-1}. The sheath temperature is 350 °C, the capillary voltage is 4.0 kV, and the fragment voltage is 150V.

The molecular formula of the compound was preliminarily predicted using the Agilent Masshunter Qualitative Analysis workstation by combining both the positive and negative excimer ion peaks. As part of the analysis and summary of component cracking law, Agilent's TCM component database was used to generate a molecular formula for selected chromatographic peaks in positive and

negative ion modes. Secondary mass spectrometry data was collected using Agilent's extraction ion stream (EIC) function.

2.3. Model of diabetes and the procedure of CUMS

An experimental model of diabetes mellitus (DM) was conducted using a high fat diet (HFD) and STZ injections (Sigma-Aldrich, St. Louis, MO, USA). A high fat diet (HFD) was administered to the rats for four weeks (58 % fat, 25 % protein, and 17 % carbohydrates, Hunan Slac Jingda Laboratory Animal Co., Ltd.), followed by the intraperitoneal administration of 60 mg kg^{-1} STZ freshly dissolved in citrate buffer (pH 4.5). Rats with fasting plasma glucose levels of 16 mmol L^{-1} were considered diabetic and further study was conducted. Based on Willner's method [12], we developed the chronic unpredictable mild stress (CUMS) model [11]. The stress procedure was conducted with a variety of stressors, including 24-h water deprivation, 2-min tail pinch, 5-min cold swimming at 4 °C, 24-h reversed light/dark cycles, 12-h food deprivation, electric shock to the foot (10 mA current; administered every other minute for 10 s, SHANDONG ACADEMY OF MEDICAL SCIENCES, YLS-9A) and noise (85 dB). The rats were exposed to CUMS for 35 days during which a stimulus was randomly selected and applied in a way that prevented them from anticipating it. A diabetes-related depression (DD) model was developed, and rats were randomly divided into four groups: the model group (DD group), a high dose of ZJJ prescription (ZJJ-H group, Table 1), a medium dose of ZJJ prescription (ZJJ-M group, Table 1), and a Metformin & Fluoxetine group (Met/F group, the dose would be 0.18 g kg^{-1} and 1.8 mg kg^{-1}, respectively). Control participants received a similar volume of normal saline. Fig. As shown in Fig. 1, the experimental procedure was followed.

2.4. Open field exploration

In order to test rodents with depressive-like behavior, an open field is commonly used (Beijing Zhongshi Science and Technology Development Co., Ltd, ZS-001). The experiment was conducted in a chamber with a diameter of 80 cm, 80 cm, and 40 cm. The area was divided into 25 equilateral squares. After 1 min of adaptation, it took 3 min to count horizontal movements (four feet within a square were counted as one score) and vertical movements. Depression is indicated by a lower score.

2.5. Morris water maze exploration (MWM)

To test spatial learning and memory, a Morris water maze (MWM, Beijing Zhongshi Science and Technology Development Co., Ltd, ZS-001) was used. A circular pool with a diameter of 1.6 m was used for recording animal activity. Four days of training were required for the rats to locate an underwater platform (2 cm). This phenomenon is known as evasive latency (EL). A shorter EL indicates better memory and learning capabilities. After the platform was removed on the fifth day, the time (in seconds) required for rats to locate the quadrants of the platform was recorded as space exploration time (SET). A longer SET indicates a greater capacity for learning and memory.

2.6. Forced swimming exploration

To detect depression-like behavior, the forced swimming test was conducted at a height of 40 cm water in a cylinder with a

Table 1
An overview of the ZJJs' components.

TCM name	English name	Manufacturer	Date of manufacture	Lot number	Contents (g)
Jianghuang	Curcuma	The First Hospital of Hunan university of Chinese Medicine	2021.10.30	2021103001	9
Danshen	Salvia miltiorrhiza	The First Hospital of Hunan university of Chinese Medicine	2021.12.25	NG21112903	12
Niuxi	Achyranthes	The First Hospital of Hunan university of Chinese Medicine	2021.12.31	SX21120317	9
Gouqi	Lycium	The First Hospital of Hunan university of Chinese Medicine	2020.01.04	HH21122801	12
Huangqi	Astragalus mongholicus	The First Hospital of Hunan university of Chinese Medicine	2021.12.15	CK21120607	18
Mudanpi	Paeonia × suffruticosa Andrews	The First Hospital of Hunan university of Chinese Medicine	2022.01.04	GK21120605	12
Shanzhuyu	Fructus corni	The First Hospital of Hunan university of Chinese Medicine	2021.12.29	SX21122003	12
Duzhong	Eucommia ulmoides	Anhui Puren Chinese Medicine slices Co., LTD	2021.06.20	2106202	9
Tusizi	Cuscuta chinensis Lam	The First Hospital of Hunan university of Chinese Medicine	2021.12.28	SX21121308	9
Shudihuang	Rehmannia glutinosa (Gaertn.) DC	Jiangsu Longfengtang Chinese Medicine Co., LTD	2021.10.05	211005420	15
Guanyelianqiao	Hypericum perforatum L	The First Hospital of Hunan university of Chinese Medicine	2021.09.27	2109270022	3

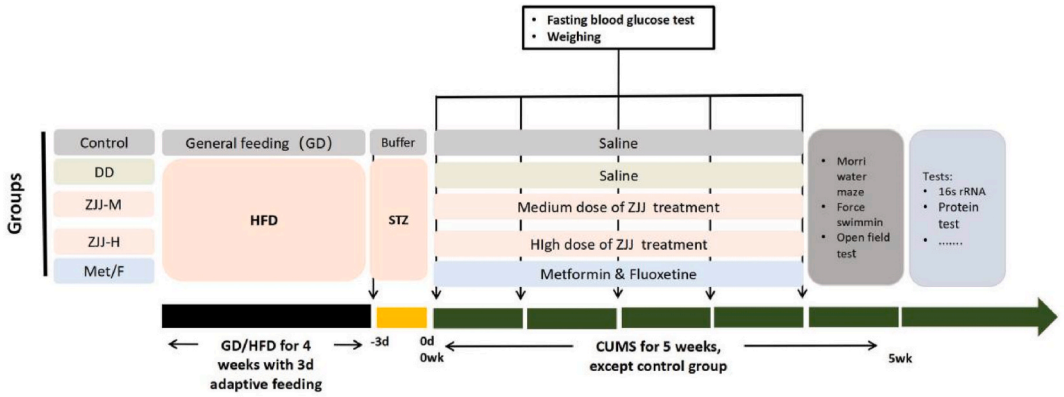

Fig. 1. The process of the experiments.

diameter of 20 cm and a height of 65 cm (Beijing Zhongshi Science and Technology Development Co.,Ltd, ZS-001). The rats were placed individually in the cylinder. Animals that were immobile were considered to be inactive. As soon as the animal became immobile within 4 min, the immobility time (in seconds) was recorded. A prolonged period of immobility is a characteristic of depression.

2.7. Enzyme-linked Immunosorbent assay (ELISA)

For the purpose of determining insulin, glycolysylated hemoglobin (GhbAh1), corticotropin-releasing hormone (CHR), adrenocorticotropic hormone (ACTH), and cortisol levels in serum and cerebrospinal fluid, ELISA kits (Jiangsu Feiya Biological Technology Co. LTD., China) were used (Sensitivity of detection for each kit: The minimum detected concentration of LPS is less than 1.0 EU.L^{-1}; The minimum detected concentration of insulin is less than 1.0 μIU.ml-1; The minimum detected concentration of IL-1β, IL-6, TNF-α, ACTH, and CRH is less than1.0 pg ml^{-1}; The minimum detected concentration of Cortisol, GhbAh1 is less than 1.0 ng ml^{-1}). In accordance with the manufacturer's instructions, a centrifuged sample was collected and stored at −80 °C for measurement. Microelisa stripplates were loaded with 10 L of samples and 40 L of diluent before being incubated at 37 °C for 60 min with HRP-conjugated reagents. Optical density was measured at 450 nm after chromogen and stop solutions were added. Meanwhile, a standard curve was prepared. HOMA-IR was calculated using the following equations:

$$\text{HOMA} - \text{IR} = \text{Nonfasting plasma} \times \frac{\text{Insulin}}{22.5}$$

2.8. Immunohistochemical test (IHC)

In accordance with previous descriptions, tissue sections of 5 mm were mounted on silanized glass slides, processed, and incubated with primary antibodies directed against TLR4 (1: 200, #AF7017, Affinity Biosciences, USA) and MyD88 (1: 200, #AF5195, Affinity Biosciences, USA). The IHC-peroxidase staining was carried out using a kit from Affinity Biosciences. In the hippocampal CA3-4 region, Images J was used to identify and count the cells that were most positive for TLR4 and MyD88.

2.9. Western Blot (WB)

The hippocampus was removed from the brain and stored at −80 °C. First, frozen tissues were lysed in an ice-cold natural lysis solution (100 mg:1000 μl, Epizyme, Column tissue protein extraction kit, PC201, China) for 5 min, followed by centrifugation for 30 s at 4 °C, 12000 rpm. Protein concentrations were determined using a BCA protein assay reagent (Solarbio science, #PC0020). Following this, the proteins were separated on polyacrylamide gels with gradients of 4–12 % (Nanjing ACE Biotechnology Co., Ltd.) before being transferred to polyvinylidene fluoride (PVDF, Millipore Corporation, USA). PVDF membranes were incubated overnight at 4 °C with the primary antibody [MyD88 (#AF5195, 1:1000) and TLR4 (#AF7017, 1:1000) antibodies were provided by Affinity Biosciences (USA); and GAPDH (#5174, 1:1000) antibodies were provided by Cell Signaling (USA)]. PVDF membranes were washed with TBST and incubated with appropriate secondary antibodies conjugated with HRP (#5127, 1:3000, Cell Signaling). The PVDF membranes were then developed using Enhanced Chemiluminescence Reagents (ECL; New Cell & Molecular Biotech, China). Following the visualization of the protein bands, the data was analyzed using an Image Lab analysis system (FluorChem R, Protein Sample, USA).

2.10. 16S rRNA sequence analysis

Samples of feces were collected for the purpose of sequencing the gut microbiota. A Rapid DNA SPIN extraction kit (MP

Biomedicals, Solon, USA) was used to extract DNA from fecal samples. To amplify and sequence the 16S ribosome V3 and V4 regions in intestinal samples (Illumina, SD, USA), PCR amplification and sequencing were used.

Trimmomatic (version 0.33) and Cutadapt (version 1.9.1) were used to identify and remove primer sequences from sequencing data. Afterwards, FLASH (version 1.2.11) was used to align the reads and to remove chimeras (UCHIME, version 8.1). This resulted in high-quality sequences that could be used for further analysis. A similarity threshold of 97 % was used to compare sequences (USEARCH, version 10.0), and an OTU threshold of 0.005 % was used to filter sequences.

The α-diversity and the β-diversity were conducted using QIIME2. The α-diversity analysis includes Chao1, Shannon, and Simpson indices. The Shannon and Simpson indices are commonly used to describe species diversity, while the Chao1 index is commonly used to describe species abundance. The β-diversity analysis was used to analyze differences between samples. In order to calculate species diversity matrices (heatmaps) and Nonmetric Multidimensional Scaling (NMDS) of the sample data, the R language platform was used. Linear discriminant analysis (LDA) was used to estimate the magnitude of the effect of abundance of each component on the effect of variance. In this analysis, the primary objective was to identify genus with significant differences in abundance between groups. Analysis of the predicted functions was conducted using KEGG signalling pathway prediction and BugBase analysis.

2.11. Statistics and analysis

The data was analyzed using GraphPad Prism 9.4. The data were presented as mean ± standard error of mean (SEM). To compare differences among three or more groups, one-way ANOVA or two-way ANOVA were used. The individual group comparisons were conducted using the Welch's *t*-test. In each group, n indicates the number of animals. Statistical significance was defined as a *p*-value less than 0.05.

3. Result

3.1. ZJJ active compounds (UPLC-Q-TOF-MS analysis of zuogui jiangtang jieyu prescription)

We previously studied Zuogui Jiangtang Jieyu prescription (ZJJ) extracts using UPLC-Q-TOF-MS to identify 57 components [13]. A total of 15 components were identified in the administered serum group, including 2-furoic acid, citric acid, gardenic acid, morroniside, loganin, cystine, millein isoflavone glycosides, salvianolic acid B, calycosin, methyl acetophenone, salvianolic acid C, carnosol, formononetin, cryptotanshinone, and tanshinone IIa.

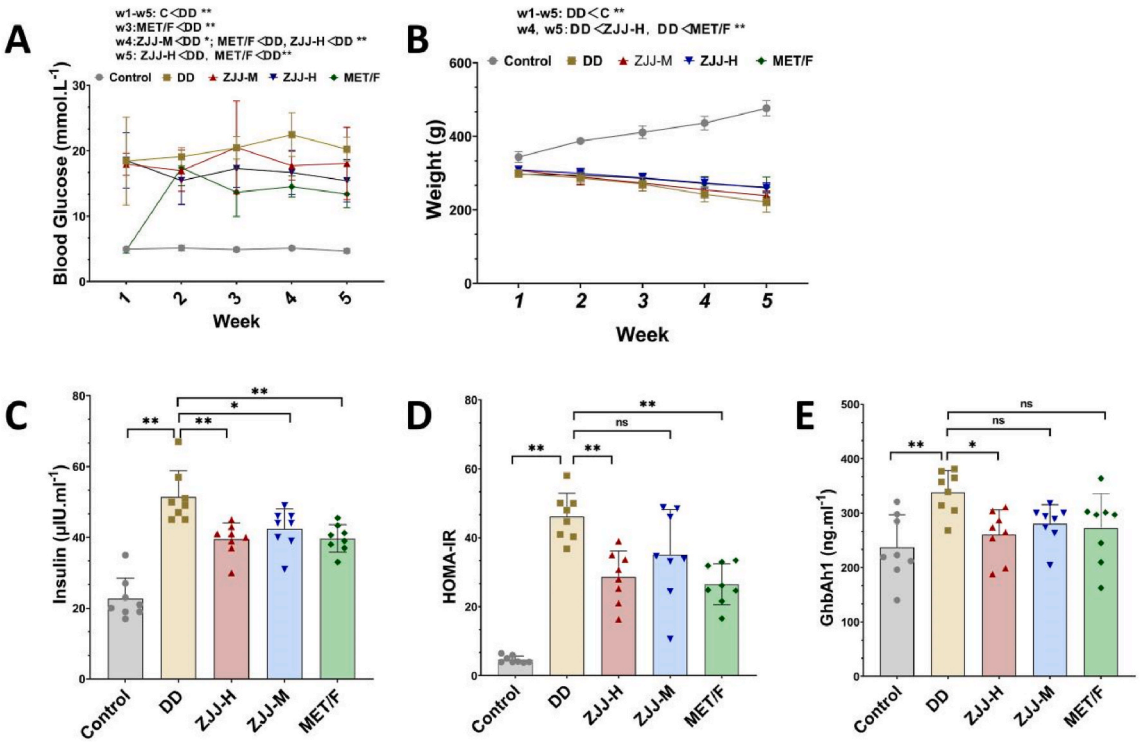

Fig. 2. Effects of ZJJ (ZJJ-M and ZJJ-H) and Met/F on glucose metabolism in DD. (A) Blood glucose levels among the groups. (B) Rats' weight gain among the groups. (C) Insulin levels for each group as determined by ELISA. (D) HOMA-IR level for each group as determined by ELISA. (E) GhbAh1 level for each group as determined by ELISA. n = 8 rats per group. The data are shown as the mean ± SEM. *p < 0.05, **p < 0.01 by ANOVA.

(Supplementary Fig. 1 & Supplementary Tab. 1).

3.2. ZJJ alleviates glucose metabolism in DD

In order to confirm the efficacy of ZJJ for DD, blood glucose, glycated haemoglobin (GhbAh1), insulin, insulin resistance (IR) and weight were measured. In Fig. 2A, the blood glucose curves of DD treated with either ZJJ (ZJJ-M and ZJJ-H) or Met/F were lower than those of the DD group, especially during the fourth and fifth weeks ($P < 0.01$, $P < 0.05$). Contrary to blood glucose, weight (Fig. 2B) exhibits the opposite pattern. DD had the lowest weight curve of the five groups, particularly during the fourth and fifth weeks ($P < 0.01$). Insulin levels (Fig. 2C), insulin resistance (Fig. 2D), and GhbAh1 levels (Fig. 2E) were significantly elevated in DD; however, these levels dramatically decreased following treatment with ZJJ-H ($P < 0.05$, $P < 0.01$) and Met/F ($P < 0.01$). The results obtained indicate that DD leads to disordered glucose metabolism and decreased weight, whereas it is alleviated by a high dose of ZJJ.

3.3. ZJJ improves depressive-like behaviour and HPA axis hyperactivity in DD

Mood disorders in DD were studied by measuring depressive-like behavior and the HPA axis. To study depression-like behavior, Morris water mazes, forced swimming tests, and open field tests are commonly used.

An assessment of learning and memory was conducted using the Morris water maze test. During the first four days, rats with a better capacity for learning spent less time locating objects underwater, and on the fifth day, rats with a better memory spent more time in the quadrant where an underwater platform had previously been located. EL (evasive latency) refers to the time taken by the rats to reach the submerged platform (Fig. 3A). During the four days of testing, EL remained highest in the DD group ($P < 0.05$, $P < 0.01$), while it gradually decreased in the other groups. In the third and fourth days, the most significant differences were observed between the DD group and the other groups. The space exploration time (SET) was significantly reduced in the DD group compared with the control group on the fifth day (Fig. 3B), and it was significantly increased after treatment with ZJJ-H ($P < 0.05$).

For the purpose of further testing depression, rats were allowed to roam freely within an 80 cm by 80 cm by 40 cm equilateral square chamber (Fig. 3C). Score the number of horizontal activities and vertical movement. According to Fig. 3C, the score was significantly decreased in DD when compared to the control ($P < 0.01$); however, i was increased in ZJJ-H ($P < 0.01$).

Forced swimming was conducted using a 65 cm tall cylinder (Fig. 3D). A positive relationship was found between depression level and immobility time in this test. According to the results obtained, rats with DD had an increased immobility time compared with the control group ($P < 0.05$), whereas it had a sharp decrease after being treated with ZJJ ($P < 0.05$).

CRH, CORT, and ACTH secretion in serum were measured to determine HPA axis function in DD (Fig. 3E–G). It appears that the levels of CRH (Fig. 3E), cortisol (Fig. 3F) and ACTH (Fig. 3G) are clearly higher in the DD group than in the control group ($P < 0.05$, $P < 0.01$), while they are notably reduced after treatment with either ZJJ-H or Met/F ($P < 0.05$).

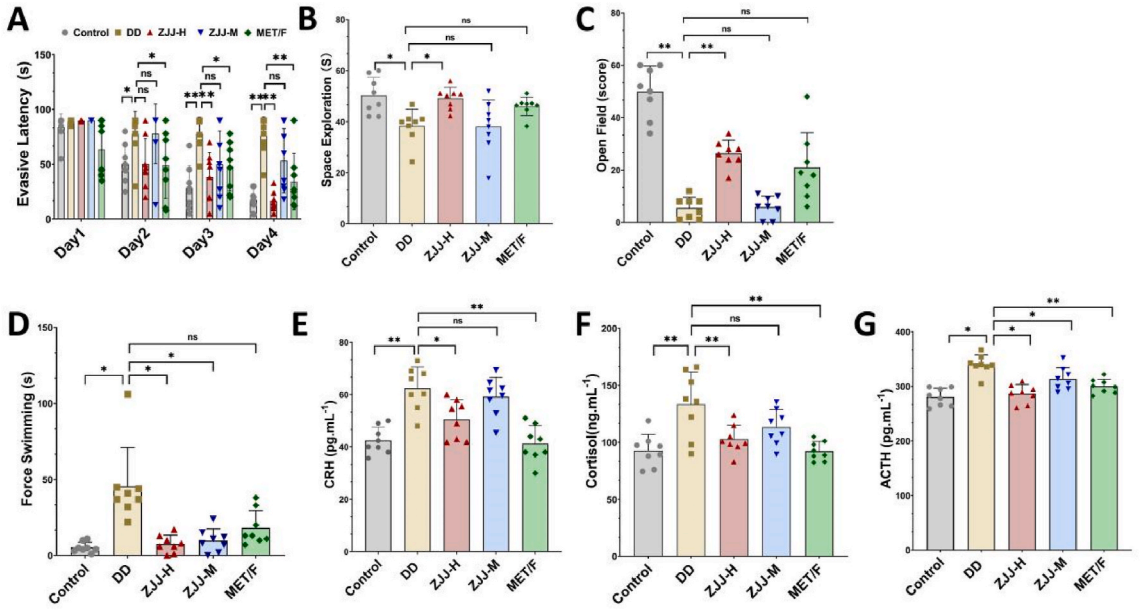

Fig. 3. Efficacy of ZJJ (ZJJ-M and ZJJ-H) and Met/F on depression-like behavior and the HPA axis in DD. (A) The evasive latency was measured in the MWM of each group. (B) The space exploration time was recorded in the MWM of each group. (C) The score of horizontal and vertical movement was performed in each group in an open field. (D) The immobility time was recorded for each group. (E–G) The levels of HPA axis-related proteins CRH, cortisol, and ACTH were measured in each group using ELISA. n = 8 rats per group. The data are shown as the mean ± SEM. *p < 0.05, **p < 0.01 by ANOVA.

3.4. ZJJ affects gut microbiota diversity in DD

The 16S rRNA sequences of faecal samples collected from each group of rats were analyzed. The α-diversity and β-diversity were assessed. The α-diversity was mainly demonstrated by three indices, namely Chao1, Shannon, and Simpson. In general, Shannon and Simpson indices are used to describe species diversity, while Chao1 is used to describe species abundance. The obtained results showed that the Chao1 (Fig. 4A), Shannon (Fig. 4B), and Simpson (Fig. 4C) indices did not significantly differ between the groups, while β-diversity refers to inter-sample differences. This study demonstrated β-diversity by the Bray–Curtis algorithm, NMDS descending dimensional analysis, and hierarchical tree diagram based on hierarchical clustering analysis. By using the Bray-Curtis algorithm, the results obtained are presented as a sample clustering heatmap with blue and red colour gradients indicating the distance between samples from near to far. A darker heatmap was observed between the DD group and the other groups, whereas a lighter heatmap was observed between the control, ZJJ-H, and ZJJ-M groups (Fig. 4D). According to NMDS descending dimensional analysis (Fig. 4E), the distance between the projection distances for control group and DD group samples was further, indicating a more diverse microbial community composition between the two groups. In addition, the projection distances between samples from the control group and the treatment groups are closely related, indicating that the microbial community composition of these groups is not entirely different. An analysis of hierarchical tree diagrams (Fig. 4F) confirmed these findings.

3.5. ZJJ changes the composition of gut microbiota in DD

The top 10 phyla and genus ranked in abundance among the top 20 phyla and genus with the smallest p-values for systematic differences in abundance between groups are presented in Fig. 5A and B. *Firmicutes* were found to be decreased in DD compared with the control, ZJJ-H and Met/F (Fig. 5A). There was, however, an increase in the abundance of *Proteobacteria, Actinobacteria, Cyanobacteria, Tenericutes, Chlorofelxi* and others in DD among the groups, particularly *Actinobacteria* and *Cyanobacteria*, which occupied almost 20 % and 7 %, respectively. According to Fig. 5B, *Ruminococcaceae* are highly expressed in the control, ZJJ, and Met/F groups, as well as *Eubacterium_coprostanoligenes*. As shown in Fig. 5C and D, *Ruminococcaceae*, *Clostridiales, Prevotellaceae,* and *Desulfovibacteriaceae* were the most dominant species in the control, whereas *Actinobacteria* dominated in the DD. The ZJJ-H showed the most influence from *Ruminococcaceae, Romboutsia, and Coprostanoligenes,* while the ZJJ-M was dominated by *Ruminococcaceae* with *Christensenellaceae.*

3.6. ZJJ decreased the level of LPS and altered the BugBase prediction in DD

In order to determine whether the gut microbiota of DD has been altered following treatment with ZJJ, 16S rRNA is used to predict the bacterial phenotype in DD. As shown in Fig. 6A–B, 6C-D, Gram-negative bacteria ($P < 0.05$) and aerobic bacteria ($P < 0.05$) were significantly more enriched in the DD group. However, they decreased after treatment with ZJJs. By contrast, DD reduced the

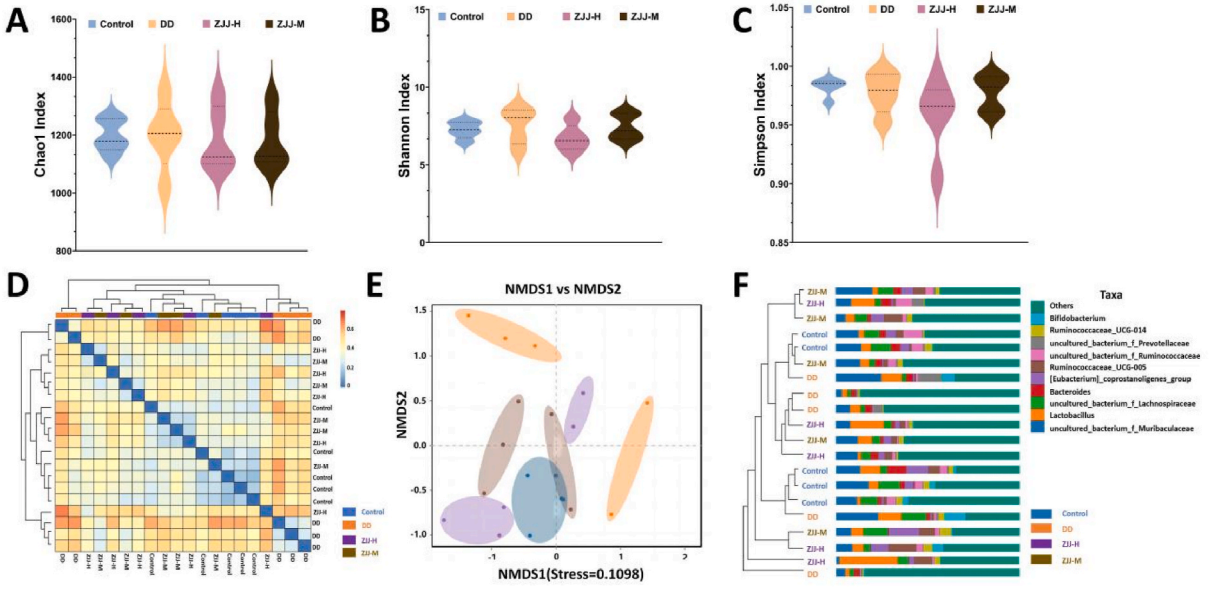

Fig. 4. The effect of ZJJ and Met/F on gut microbiota disorder in DD. (A) The Chao1 diversity index for each group. (B) The Shannon diversity index for each group. (C) The Simpson diversity index for each group. (D) Based on the sample clustering heatmap, the Bray-Curtis algorithm was used to analyze differences between groups across samples. (E) The differences between groups were analyzed using NMDS descending dimensional analysis. (F) Hierarchical tree diagrams based on hierarchical clustering were used to analyze the differences between samples between groups. n = 5 rats per group.

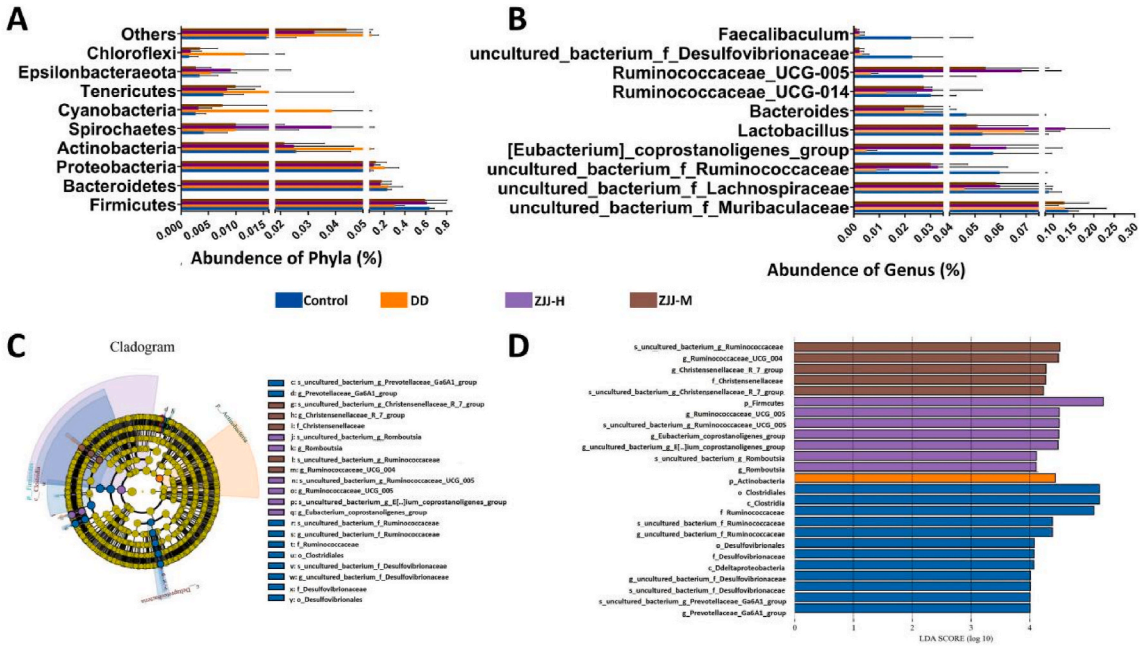

Fig. 5. The composition of the gut microbiota in DD is changed by ZJJ and Met/F. (A) Differences between the bacterial phyla of the groups. (B) Differences between bacterial genera of the groups. (C) Cladogram analysis of microbiota biomarkers in each group. (D) Biomarkers of microbiota between groups based on line discriminant analysis. n = 5 rats per group.

abundance of anaerobic bacteria significantly (Fig. 6E and F) ($P < 0.05$), but rebounded after ZJJ treatments were administered. As shown in Fig. 6G and HA, a large number of biofilm-forming bacteria were found in DD ($P < 0.05$), almost several times greater than those found in controls. Additionally, LPS, an important component of Gram-negative bacterial cell walls, was examined in the serum of each group (Fig. 6I). The obtained results were consistent with the abundance of Gram-negative bacteria in each group.

3.7. ZJJ influences the predictive microbial functional profiling

Using 16S rRNA datasets, STAMP can be used to predict the functions of microbial communities. In our study, we employed STAMP analysis to determine the functional profiles of communities across groups. A significantly higher proportion of organism systems and human disease-related sequences ($P < 0.05$) were found in DD (Fig. 7A), whereas ZJJ showed a significantly lower proportion ($P < 0.05$) (Fig. 7B). Level 2 analysis revealed that 10 pathways [endocrine system ($P < 0.01$), cell growth and death ($P < 0.01$), infectious disease: bacteria ($P < 0.01$), infectious disease: parasitic ($P < 0.01$), metabolism of other amino acids ($P < 0.01$), transport and catabolism ($P < 0.05$), lipid metabolism ($P < 0.05$), drug resistance antineoplastic ($P < 0.05$), metabolism of terpenoids and polyketides ($P < 0.05$) and infectious disease: viral ($P < 0.05$)] were significantly enriched in the DD group compared with the control group, while 3 pathways [immune system ($P < 0.01$), nervous system ($P < 0.05$) and environmental adaptation ($P < 0.05$)] were significantly increased in the control group (Fig. 7C). As well as this, four pathways (Fig. 7D) differed significantly between ZJJ-H and DD, including the endocrine system pathway ($P < 0.01$), transport and catabolism pathway ($P < 0.05$), metabolism of other amino acids pathway ($P < 0.05$), and folding, sorting and degradation pathway ($P < 0.05$).

3.8. ZJJ relieves inflammation in the brain and inhibits TLR4/MyD88 signalling pathway activation in the hippocampal CA3 region in DD

The effects of ZJJ on neuroprotection and anti-inflammatory activity in DD were further assessed by detecting inflammatory cytokines in cerebrospinal fluid, morphological changes in hippocampal neurons, and TLR4/MyD88 protein expression by IHC staining and Western Blot. The obtained results indicated that the level of IL-1β (Fig. 8A), IL-6 (Fig. 8B), and TNF-α (Fig. 8C) in cerebrospinal fluid was increased in DD compared with the control ($P < 0.01$), while they were significantly decreased after treatment with ZJJ-H and ZJJ-M ($P < 0.01$, $P < 0.05$). Furthermore, the pyramidal neurons in the hippocampal CA3 area of the control group were almost firmly sorted in the order shown in Fig. 8D and F. Generally, the neurons exhibited a typical microstructure, a clear shape, and a moderate size. The DD group, however, showed neuronal shrinkage and loss as well as cytoplasmic pyknosis. With ZJJ treatment, neurons gradually recovered in DD. IHC results indicated an increase in TLR4-positive ($P < 0.05$) and MyD88-positive ($P < 0.01$) cells in the DD group compared to the control group in terms of protein expression of TLR4 and MyD88 (Fig. 8E and G). In contrast, ZJJ-H therapy significantly reduced TLR4 ($P < 0.05$) and MyD88-positive cells ($P < 0.01$). Furthermore, Western blots were performed to assess the expression of TLR4 and MyD88 in the hippocampus (Fig. 8H–J). According to the results, the expression of TLR4 (Fig. 8I) and MyD88 (Fig. 8J) was increased in DD when compared to the control group ($P < 0.01$), and they were dramatically decreased after

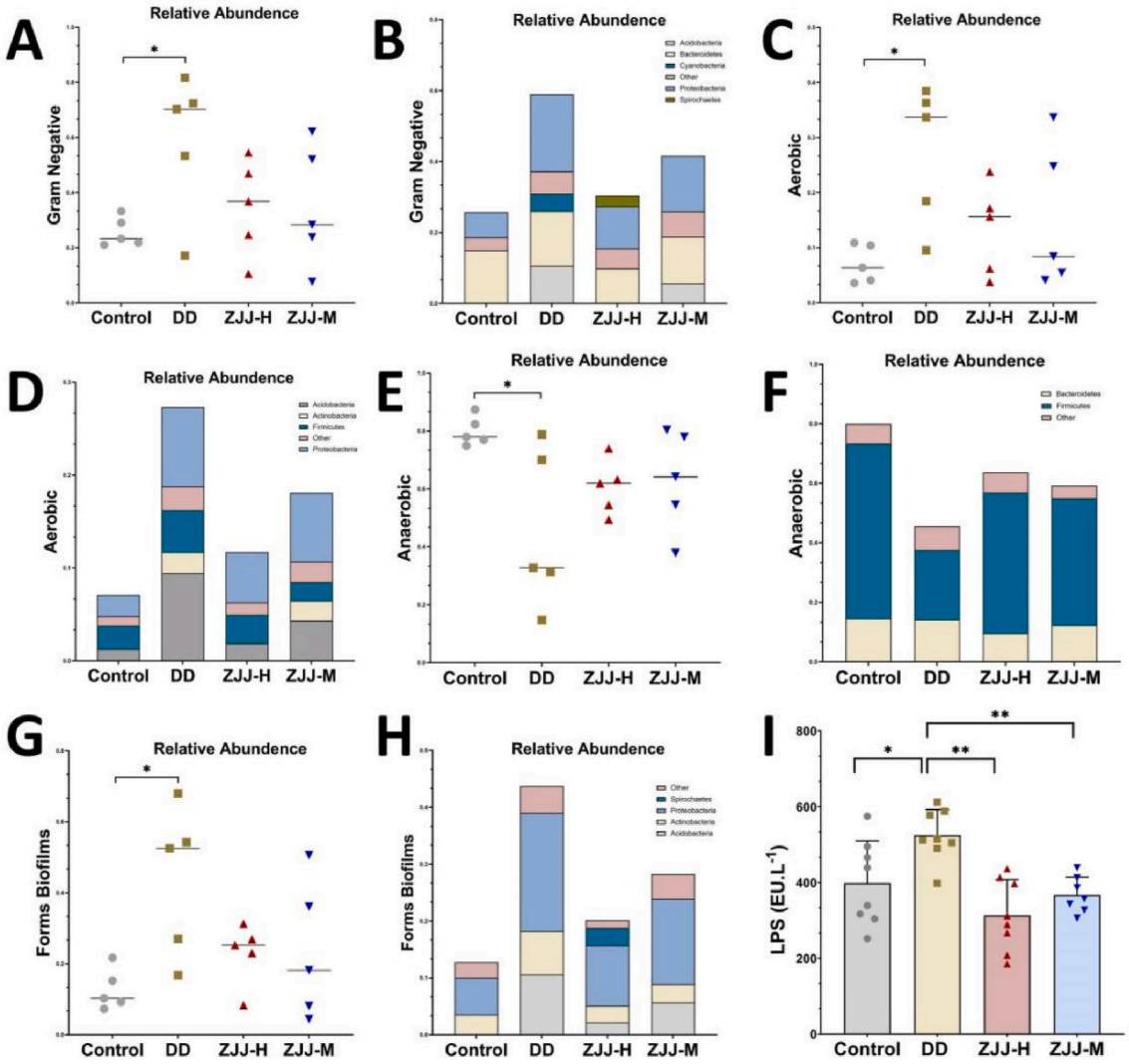

Fig. 6. The level of LPS (n = 8/group) in serum and the BugBase prediction (n = 5/group) in DD. (A–B) Predicted abundance of Gram-negative bacteria with its phylum in each group. (C–D) Predicted abundance of aerobic bacteria with its phylum in each group. (E–F) Predicted abundance of anaerobic bacteria with its phylum in each group. (G–H) Predicted abundance of biofilm formation ability with its phylum in each group. (I) The LPS level for each group in serum (n = 8/group). The data are shown as the mean ± SEM. $^{*}p < 0.05$, $^{**}p < 0.01$ by *ANOVA*.

receiving ZJJs.

4. Discussion

In order to establish a rat model of diabetes-related depression, a high-fat diet (HFD) was followed by STZ injections and stress administration (CUMS) for five weeks. DD rats displayed significant weight loss and increased blood glucose levels, along with abnormal HOMA-IR and GhbAh1 levels, indicating severe glucose metabolism disorders in this model, as well as depression-like behavior associated with HPA axis hyperactivity. Thus, it appears that a model of diabetes-related depression has been successfully developed. ZJJ, which nourishes Yin and benefits Qi, resolves stasis and alleviates depression, as well as reducing neuroinflammation, has been shown to be beneficial in treating DD in our previous studies. A biological process underlying ZJJ treatment for DD was examined in this study. It involved improving gut microbiota and alleviating neuroinflammation (inhibition of hippocampal TLR4/MyD88 signaling pathways and alleviation of neuroinflammation, thus protecting the hippocampus). The ZJJ treatment of DD has also been demonstrated to be multi-level and multi-targeted. Further studies with a larger sample size and better protocols are needed to determine whether the improvements in gut mocrobiota and neuroinflammation caused by ZJJ in this study are caused by the brain-gut axis.

Previous studies on the treatment of DD with ZJJ focused on clinical studies, neurological functions, and endocrine and metabolic functions [14,15]. There has been considerable interest in the use of traditional Chinese medicine to improve gut microbiota in recent

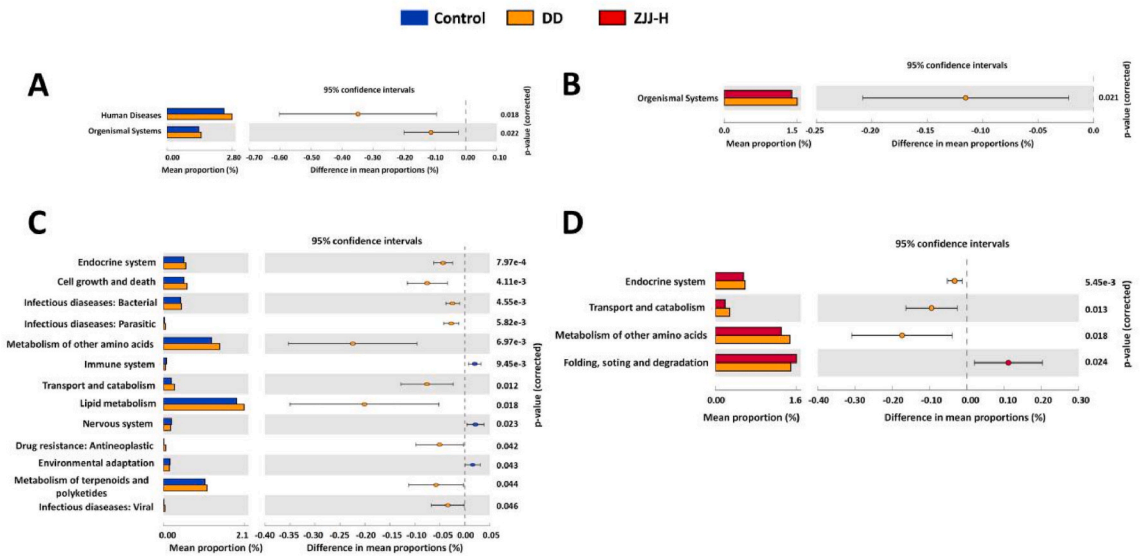

Fig. 7. KEGG signaling pathways were compared between groups, including control with DD, DD with ZZJ-H. (A) Prediction of KEGG signaling pathways between control and DD at level 1. (B) Prediction of KEGG signaling pathways between DD and ZJJ-H at level 1. (C) Prediction of KEGG signaling pathways between control and DD at level 2. (D) Prediction of KEGG signaling pathways between DD and ZJJ-H at level 2.

years, which has been shown to improve glucose metabolism and depression-like behavior [16–18]. Although the effects of ZJJ on gut microbiota are unknown, multiple studies have demonstrated its effectiveness in treating diabetes-related depression [3,4,19]. The present study found that the gut microbiota of the DD group differed significantly from that of the control group and improved following the administration of a high dose of ZJJ (Figs. 4–5). Many studies have shown that ZJJ contains several herbs that are capable of improving gut microbiota in a variety of ways, including antidepressant effects and glucose metabolism effects, including Salvia miltiorrhiza, turmeric, and prepared radix rehmanniae. The presence of these herbs affects the ratio between Bacteroidetes and Firmicutes in the gut microbiota [20–22]. It has also been demonstrated that Astragalus membranaceus and Lycium improve glucose metabolism by increasing short-chain fatty acid synthesis [23,24], inhibiting hippocampal apoptosis, and providing antidepressant effects.as well as inhibiting the apoptosis of hippocampal neurons and providing antidepressant effects [25]. Our previous study of ZJJ's chemical composition indicated that its main source of extracts was Astragalus membranaceus, Salvia miltiorrhiza, and Lycium (Supplementary Fig. 1). Thus, it is hypothesized that ZJJ could effectively improve gut microbiota, offering a possible new therapeutic target for DD.

Recent studies have found that diabetes with cognitive disorders is closely related to neuroinflammation [26]. The proinflammatory cytokines such as tumour necrosis factor (TNF), IL-1, IL-2, and IL-6 are overexpressed in the brain in patient with diabetes and Alzheimer's disease, suggesting a role for inflammation in neuronal damage [27]. There are several possible effects of persistent inflammation, including changes in neurotransmission, changes in neurogenesis, and damage to neurons [28].The dysbiosis of the gut microbiota contributes to neuroinflammation through the microbiota-gut-brain axis, resulting in an increased abundance of Gram-negative bacteria in the gut [29]. Gram-negative bacteria were found to be significantly more abundant in DD in this study. And gram-negative bacteria produce LPS, which is considered to be a proinflammatory agent [30]. By contributing to the formation of biofilms, certain Gram-negative bacteria may increase exposure to LPS [31], which is consistent with our prediction that biofilm formation-associated bacteria were increased in DD and downregulated after treatments (Fig. 7). A previous study conducted by our group demonstrated that probiotics improved the gut microbiota of DD rats, which resulted in a significant reduction in blood glucose, an improvement in LPS and pro-inflammatory cytokines, and a significant reduction in depressive-like behavior and hyperHPA [32]. There was evidence that ZJJ improved the gut microbiota of DD patients, resulting in lower levels of LPS in serum and TNF-α, IL-1 and IL-6 in cerebrospinal fluid. We conclude that neuroinflammation in DD is closely related to gut microbiota disorders, and ZJJ can effectively improve gut microbiota of DD and alleviate neuroinflammation.

In addition, LPS reacts with TLR4 and activates the MyD88 pathway, which leads to the production of proinflammatory cytokines [17,29]. Hippocampal neurons contain a TLR4-regulated MyD88-dependent pathway [33], and the activation of this pathway increases the expression of proinflammatory factors such as TNF-α and IL-1β in cells [34]. Hippocampus neuronal damage is closely associated with proinflammatory factors in the brain [35]. According to the present study, TLR4 and MyD88 are highly expressed in the hippocampus (Fig. 8D–J), while they are decreased following treatment with ZJJ. Further, LPS levels were high in DD serum, but decreased after treatment with ZJJ (Fig. 6I). ZJJ's active ingredient may improve the development of DD by inhibiting the TLR4/MyD88 signalling pathway, which is believed to be closely related to the development of DD. ZJJ's active ingredient has the potential to modulate this pathway through inhibition of LPS in order to mitigate the development of DD. The TLR4/MyD88 pathway was found to be regulated by some herbal monomers in ZJJ. Salvianolic acid [36], mortoriciside [37], formononetin [38], and Loganin [39] found in the drug-containing serum of ZJJ inhibit the expression of MyD88, NF-κB, IL-1β and IL-6 in the TLR4-mediated signaling

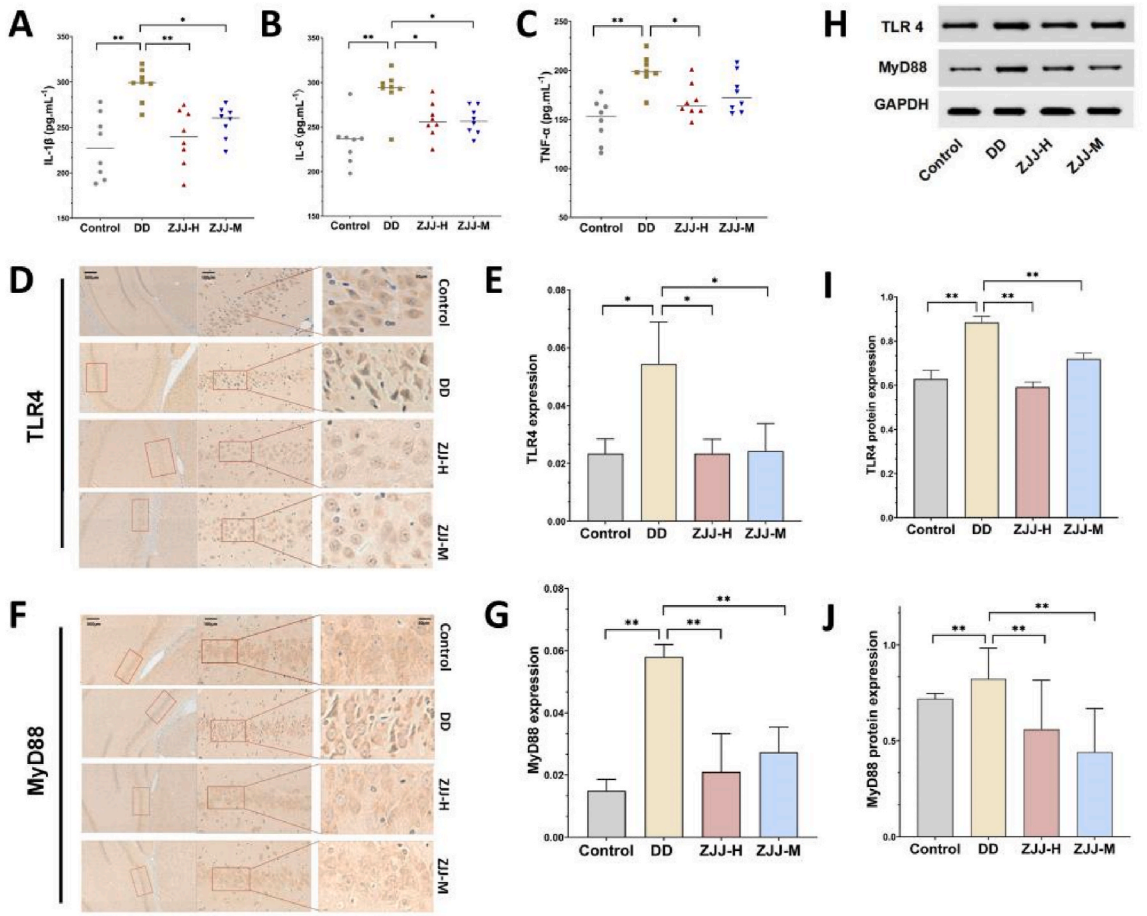

Fig. 8. ZJJ affected the TLR4/MyD88 signalling pathway in hippocampal Ca3 in DD, as well as proinflammatory cytokines detected by ELISA. (A) The level of IL-1β in cerebrospinal fluid was assessed by ELISA (n = 8/group). (B) The level of IL-6 in cerebrospinal fluid was assessed by ELISA (n = 8/group). (C) The level of TNF-α in cerebrospinal fluid was assessed by ELISA (n = 8/group). (D–G) The expression of TLR4 and MyD88 in hippocampal CA3-4 of each group was measured by immunohistochemistry (n = 3/group); (H) Western blots were performed to assess the expression of TLR4, MyD88, and GAPDH in hippocampal CA3-4. (I) Quantitative analysis of TLR4 expression (n = 4/group). (J) Quantitative analysis of MyD88 expression (n = 4/group). The IHC and WB method evaluated protein expression. The data are shown as the mean ± SEM. *$p < 0.05$, **$p < 0.01$ by ANOVA.

pathway. ZJJ therefore reduces LPS levels by improving gut microbiota and inhibiting hippocampal TLR4/myd88 signaling pathways, thus reducing inflammatory factors and alleviating hippocampal neurodegeneration.

It is thus concluded that the multilevel and multi-target treatment of DD by ZJJ is not only reflected in improvements in nerve function, endocrine metabolism and other functions, but also in the improvement of intestinal flora disorder and the alleviation of hippocampal neuron damage. It is still necessary to conduct further experiments in order to determine the exact mechanism.

5. Conclusion

We conclude that the gut microbiota of DD rats is altered and affects several microbial community functions, including the endocrine system, immune system, and nervous system (Fig. 7), which are strongly associated with neuroinflammation in DD development. Through multi-level and multi-target treatment, ZJJ can effectively improve glucose metabolism and depression-like behaviors in DD patients. And there was an improvement in gut microbiota as well as regulation of the TLR4/MyDD88 signaling pathway in the hippocampal tissue. Certainly, the improvement of gut microbiota is associated with the TLR4/myd88 signaling pathway, but further research is needed to determine whether improvements in gut microbiota and neuroinflammation brought about by ZJJ in this study are caused by the brain-gut axis.

CRediT authorship contribution statement

Li Wei: Writing – review & editing, Writing – original draft, Funding acquisition, Formal analysis, Data curation. **Yang Hui:**

Writing – review & editing, Funding acquisition, Formal analysis, Data curation. **Wang Jinxi:** Methodology, Formal analysis. **Lei Shihui:** Methodology, Formal analysis. **Long Hongping:** Formal analysis. **Liu Jian:** Funding acquisition, Formal analysis, Data curation. **Liu Lin:** Supervision, Project administration, Investigation, Funding acquisition.

Availability of data and materials

16s sRNA sequencing reads were deposited in the short read archive of NCBI under SRA number SRP387996.

Declaration of competing interest

The authors declare that they have no known competing financial interests or personal relationships that could have appeared to influence the work reported in this paper.

Appendix A. Supplementary data

Supplementary data to this article can be found online at https://doi.org/10.1016/j.heliyon.2024.e39291.

References

[1] N. Sartorius, Depression and diabetes, Dialogues Clin. Neurosci. 20 (2018) 47–52, https://doi.org/10.31887/DCNS.2018.20.1/nsartorius.
[2] Huizhen Zhang, Li Tingting, Li Wei, et al., Research progress of comorbidity mechanism and TCM treatment of diabetes mellitus with depression and anxiety disorder, Chinese Rural Medicine 30 (2023) 75–77.
[3] S.C. Ng, Z. Xu, J.W.Y. Mak, K. Yang, Q. Liu, T. Zuo, W. Tang, Microbiota engraftment after faecal microbiota transplantation in obese subjects with type 2 diabetes: a 24-week, double-blind, randomised controlled trial, Gut (2022) 716–723.
[4] P. Tian, Y. Chen, H. Zhu, L. Wang, X. Qian, R. Zou, Bifidobacterium breve CCFM1025 attenuates major depression disorder via regulating gut microbiome and tryptophan metabolism: a randomized clinical trial, Brain Behav. Immun. 100 (2022) 233–241, https://doi.org/10.1016/j.bbi.2021.11.023.
[5] Y. Cheng, Z. Ling, L. Li, The intestinal microbiota and colorectal cancer, Front. Immunol. 11 (2020) 615056, https://doi.org/10.3389/fimmu.2020.615056.
[6] H.R. Peng, J.Q. Qiu, Q.M. Zhou, et al., Intestinal epithelial dopamine receptor signaling drives sex-specific disease exacerbation in a mouse model of multiple sclerosis, Immunity 56 (2023) 2773–2789, https://doi.org/10.1016/j.immuni.2023.10.016.
[7] S. Carloni, M. Rescigno, The gut-brain vascular axis in neuroinflammation, Semin. Immunol. 69 (2023) 101802, https://doi.org/10.1016/j.smim.2023.101802.
[8] G. Zhu, J. Zhao, H. Zhang, G. Wang, W. Chen, Gut microbiota and its metabolites: bridge of dietary nutrients and alzheimer's disease, Adv. Nutr. 14 (2023) 819–839, https://doi.org/10.1016/j.advnut.2023.04.005.
[9] Ping Li, Yang Liu, Manshu Zou, et al., Neuroprotective effect and mechanism of Zuogui Jiangtang Jieyu Formula on diabetes mellitus complicated with depression model rats based on CX3CL1-CX3CR1 axis, Zhongguo Zhongyao Zazhi 48 (2023) 5822–5829, https://doi.org/10.19540/j.cnki.cjcmm.20230605.406.
[10] Z. Zhao, Fecal Microbiota Transplantation Protects Rotenone-Induced Parkinson's Disease Mice via Suppressing Inflammation Mediated by the Lipopolysaccharide-TLR4 Signaling Pathway through the Microbiota-Gut-Brain axis, 2021, p. 27.
[11] D. Karaiskos, E. Tzavellas, I. Ilias, I. Liappas, T. Paparrigopoulos, Agomelatine and sertraline for the treatment of depression in type 2 diabetes mellitus, Int. J. Clin. Pract. 67 (2013) 257–260, https://doi.org/10.1111/ijcp.12112.
[12] Y.-H. Wang, L.-T. Yin, H. Yang, X.-L. Li, K.-G. Wu, Hypoglycemic and anti-depressant effects of Zuogui Jiangtang Jieyu formulation in a model of unpredictable chronic mild stress in rats with diabetes mellitus, Exp. Ther. Med. 8 (2014) 281–285, https://doi.org/10.3892/etm.2014.1681.
[13] Z.H.A.N.G. Chi, Z.H.O.U. Siqian, Long, Long Hongping, In vitro and in vivo components analysis of Zuogui Jiangtang Jieyu prescription based on UPLC-Q-TOF-MS, Tradit Chin Drug Res Pharmacol 34 (2023).
[14] Xiuli Zhang, Yuhong Wang, hui Yang, Meng Pan, Effects of Zuogui Jiangtangjieyu Prescription on learning and memory and hippocampal ultrastructure in diabetic model rats with depression, Shi Zhen Traditional Chinese Medicine 26 (4) (2015).
[15] Zhao Hongqing, Qing Du, Ling Jia, et al., Effects of Zuogui Jiangtangjieyu Prescription on JNK/ELK-1/C-fos pathway in hippocampal neurons of diabetic depression rats, Chin. J. Clin. Pharmacol. Therapeut. 21 (6) (2016).
[16] Y. Zheng, Q. Ding, Y. Wei, X. Gou, J. Tian, M. Li, X. Tong, Effect of traditional Chinese medicine on gut microbiota in adults with type 2 diabetes: a systematic review and meta-analysis, Phytomedicine 88 (2021) 153455, https://doi.org/10.1016/j.phymed.2020.153455.
[17] S. Shao, R. Jia, L. Zhao, Y. Zhang, Y. Guan, H. Wen, J. Liu, Y. Zhao, Y. Feng, Z. Zhang, Q. Ji, Q. Li, Y. Wang, Xiao-Chai-Hu-Tang ameliorates tumor growth in cancer comorbid depressive symptoms via modulating gut microbiota-mediated TLR4/MyD88/NF-κB signaling pathway, Phytomedicine 88 (2021) 153606, https://doi.org/10.1016/j.phymed.2021.153606.
[18] L. Lin, L. Luo, M. Zhong, T. Xie, Y. Liu, H. Li, J. Ni, Gut microbiota: a new angle for traditional herbal medicine research, RSC Adv. 9 (2019) 17457–17472, https://doi.org/10.1039/C9RA01838G.
[19] Y. Wang, H. Yang, W. Li, P. Meng, Y. Han, X. Zhang, D. Cao, Y. Tan, Zuogui Jiangtang Jieyu formulation prevents hyperglycaemia and depressive-like behaviour in rats by reducing the glucocorticoid level in plasma and Hippocampus, Evid. base Compl. Alternative Med. 2015 (2015) 1–10, https://doi.org/10.1155/2015/158361.
[20] F. Zhang, Y. Xu, L. Shen, J. Huang, S. Xu, J. Li, Z. Sun, J. He, M. Chen, Y. Pan, GuanXinNing tablet attenuates alzheimer's disease via improving gut microbiota, host metabolites, and neuronal apoptosis in rabbits, Evid. base Compl. Alternative Med. 2021 (2021) 1–20, https://doi.org/10.1155/2021/9253281.
[21] J. Sun, Q. Wu, H. Xu, The herb pair radix rehmanniae and cornus officinalis attenuated testicular damage in mice with diabetes mellitus through butyric acid/glucagon-like peptide-1/glucagon-like peptide-1 receptor pathway mediated by gut microbiota, Front. Microbiol. 13 (2022) 15.
[22] C. Yang, Y. Du, D. Ren, X. Yang, Y. Zhao, Gut microbiota-dependent catabolites of tryptophan play a predominant role in the protective effects of turmeric polysaccharides against DSS-induced ulcerative colitis, Food Funct. 12 (2021) 9793–9807, https://doi.org/10.1039/D1FO01468D.
[23] J. Gu, R. Sun, Q. Wang, F. Liu, D. Tang, X. Chang, Standardized Astragalus mongholicus bunge-curcuma aromatica salisb. Extract efficiently suppresses colon cancer progression through gut microbiota modification in CT26-bearing mice, Front. Pharmacol. 12 (2021) 714322, https://doi.org/10.3389/fphar.2021.714322.
[24] Y. Yang, Y. Chang, Y. Wu, H. Liu, Q. Liu, Z. Kang, M. Wu, H. Yin, J. Duan, A homogeneous polysaccharide from Lycium barbarum: structural characterizations, anti-obesity effects and impacts on gut microbiota, Int. J. Biol. Macromol. 183 (2021) 2074–2087, https://doi.org/10.1016/j.ijbiomac.2021.05.209.
[25] F. Zhao, S. Guan, Y. Fu, K. Wang, Z. Liu, T.B. Ng, Lycium barbarum polysaccharide attenuates emotional injury of offspring elicited by prenatal chronic stress in rats via regulation of gut microbiota, Biomed. Pharmacother. 143 (2021) 112087, https://doi.org/10.1016/j.biopha.2021.112087.

[26] H. Ehtewish, A. Arredouani, O. El-Agnaf, Diagnostic, prognostic, and mechanistic biomarkers of diabetes mellitus-associated cognitive decline, IJMS 23 (2022) 6144, https://doi.org/10.3390/ijms23116144.
[27] J.M. Gaspar, F.I. Baptista, M.P. Macedo, A.F. Ambrósio, Inside the diabetic brain: role of different players involved in cognitive decline, ACS Chem. Neurosci. 7 (2016) 131–142, https://doi.org/10.1021/acschemneuro.5b00240.
[28] A.L. Soung, A. Vanderheiden, A.S. Nordvig, et al., COVID-19 induces CNS cytokine expression and loss of hippocampal neurogenesis, Brain 145 (2022).
[29] L. Huang, C. Thonusin, N. Chattipakorn, S.C. Chattipakorn, Impacts of gut microbiota on gestational diabetes mellitus: a comprehensive review, Eur. J. Nutr. 60 (2021) 2343–2360, https://doi.org/10.1007/s00394-021-02483-6.
[30] M. Rajilić-Stojanović, W.M. de Vos, The first 1000 cultured species of the human gastrointestinal microbiota, FEMS Microbiol. Rev. 38 (2014) 996–1047, https://doi.org/10.1111/1574-6976.12075.
[31] I. Hetemäki, C. Jian, S. Laakso, O. Mäkitie, A.-M. Pajari, W.M. de Vos, T.P. Arstila, A. Salonen, Fecal bacteria implicated in biofilm production are enriched and associate to gastrointestinal symptoms in patients with apeced – a pilot study, Front. Immunol. 12 (2021) 668219, https://doi.org/10.3389/fimmu.2021.668219.
[32] Shihui Lei, Li Wei, Yang Hui, et al., Effects of probiotics on blood glucose and depression-like behavior in rats with diabetes-related depression by regulating gut microbiota, Chin J Diabetes Mellitus 14 (2022) 1453–1460.
[33] M.R. Dasu, S. Devaraj, S. Park, I. Jialal, Increased toll-like receptor (TLR) activation and TLR ligands in recently diagnosed type 2 diabetic subjects, Diabetes Care 33 (2010) 861–868, https://doi.org/10.2337/dc09-1799.
[34] C. Cheng, L. Zhang, J. Mu, Q. Tian, Y. Liu, X. Ma, Y. Fu, Z. Liu, Z. Li, Effect of lactobacillus johnsonii strain SQ0048 on the TLRs-MyD88/NF-κB signaling pathway in bovine vaginal epithelial cells, Front. Vet. Sci. 8 (2021) 670949, https://doi.org/10.3389/fvets.2021.670949.
[35] B. Zhang, W. Lian, J. Zhao, Z. Wang, A. Liu, G. Du, DL0410 alleviates memory impairment in D-galactose-induced aging rats by suppressing neuroinflammation via the TLR4/MyD88/NF-κB pathway, Oxid. Med. Cell. Longev. 2021 (2021) 1–31, https://doi.org/10.1155/2021/6521146.
[36] H. Shi, P. Zhou, G. Gao, Astragaloside IV prevents acute myocardial infarction by inhibiting the TLR4/MyD88/NF-κB signaling pathway, J. Food Biochem. 45 (7) (2021) 10.
[37] C. Park, H.J. Cha, H. Lee, et al., The regulation of the TLR4/NF-κB and Nrf2/HO-1 signaling pathways is involved in the inhibition of lipopolysaccharide-induced inflammation and oxidative reactions by morroniside in RAW 264.7 macrophages, Arch. Biochem. Biophys. (2021), https://doi.org/10.1016/j.abb.2021.108926.
[38] J. Wang, L. Wang, J. Zhou, et al., The protective effect of formononetin on cognitive impairment in streptozotocin (STZ)-induced diabetic mice, Zhou J 106 (2018) 1250–1257, https://doi.org/10.1016/j.biopha.2018.07.063.
[39] Y. Cui, Y. Wang, D. Zhao, et al., Loganin prevents BV-2 microglia cells from Aβ1-42 -induced inflammation via regulating TLR4/TRAF6/NF-κB axis, Cell Biol. Int. 42 (2018) 1632–1642, https://doi.org/10.1002/cbin.11060.